Published in final edited form as:

J Am Chem Soc. 2021 April 21; 143(15): 6006–6017. doi:10.1021/jacs.1c02150.

Total Synthesis and Computational Investigations of Sesquiterpene-Tropolones Ameliorate Stereochemical Inconsistencies and Resolve an Ambiguous Biosynthetic Relationship

Christopher Y. Bemis[‖],
Roger Adams Laboratory, Department of Chemistry, University of Illinois, Urbana, Illinois 61801, United States; Cancer Center at Illinois, University of Illinois, Urbana, Illinois 61801, United States

Chad N. Ungarean[‖],
Roger Adams Laboratory, Department of Chemistry, University of Illinois, Urbana, Illinois 61801, United States; Cancer Center at Illinois, University of Illinois, Urbana, Illinois 61801, United States

Alexander S. Shved,
Roger Adams Laboratory, Department of Chemistry, University of Illinois, Urbana, Illinois 61801, United States; Cancer Center at Illinois, University of Illinois, Urbana, Illinois 61801, United States

Cooper S. Jamieson,
Department of Chemistry and Biochemistry, University of California, Los Angeles, California 90095, United States

Taehwan Hwang,
Roger Adams Laboratory, Department of Chemistry, University of Illinois, Urbana, Illinois 61801, United States; Cancer Center at Illinois, University of Illinois, Urbana, Illinois 61801, United States

Ken S. Lee,
Roger Adams Laboratory, Department of Chemistry, University of Illinois, Urbana, Illinois 61801, United States; Cancer Center at Illinois, University of Illinois, Urbana, Illinois 61801, United States

K. N. Houk,
Department of Chemistry and Biochemistry, University of California, Los Angeles, California 90095, United States

David Sarlah

Corresponding Author: David Sarlah – Roger Adams Laboratory, Department of Chemistry, University of Illinois, Urbana, Illinois 61801, United States; Cancer Center at Illinois, University of Illinois, Urbana, Illinois 61801, United States; sarlah@illinois.edu.
[‖]C.Y.B. and C.N.U. contributed equally.

Supporting Information
The Supporting Information is available free of charge at https://pubs.acs.org/doi/10.1021/jacs.1c02150.
Detailed experimental procedures, spectroscopic data, computational data, and ^{1}H and ^{13}C NMR spectra (PDF)

Accession Codes
CCDC 2050423–2050428 contain the supplementary crystallographic data for this paper. These data can be obtained free of charge via www.ccdc.cam.ac.uk/data_request/cif, or by emailing data_request@ccdc.cam.ac.uk, or by contacting The Cambridge Crystallographic Data Centre, 12 Union Road, Cambridge CB2 1EZ, UK; fax: +44 1223 336033.

Complete contact information is available at: https://pubs.acs.org/10.1021/jacs.1c02150

The authors declare no competing financial interest.

Roger Adams Laboratory, Department of Chemistry, University of Illinois, Urbana, Illinois 61801, United States; Cancer Center at Illinois, University of Illinois, Urbana, Illinois 61801, United States

Abstract

The sesquiterpene-tropolones belong to a distinctive structural class of meroterpene natural products with impressive biological activities, including anticancer, antifungal, antimalarial, and antibacterial. In this article, we describe a concise, modular, and cycloaddition-based approach to a series of sesquiterpene mono- and bistropolones, including (−)-epolone B, (+)-isoepolone B, (±)-dehydroxypycnidione, and (−)-10-*epi*-pycnidione. Alongside the development of a general strategy to access this unique family of metabolites were computational modeling studies that justified the diastereoselectivity observed during key cycloadditions. Ultimately, these studies prompted stereochemical reassignments of the pycnidione subclass and shed additional light on the biosynthesis of these remarkable natural products.

Graphical Abstract

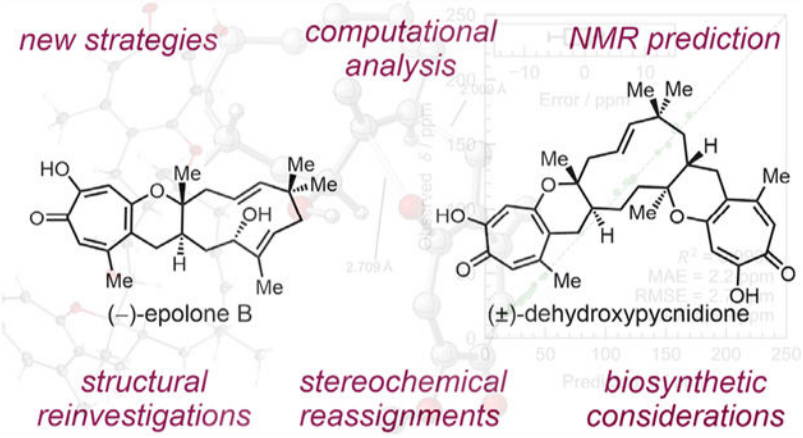

INTRODUCTION

The sesquiterpene-tropolones are a unique subset of meroterpenes, with pycnidione (**1′**, Figure 1a) serving as the first representative member to be isolated from cultures of *Phoma sp.* (MF 4728) in 1993.[1] With other tropolone-containing natural products[2–6] and compounds[7–14] boasting impressive bioactivities, pycnidione follows suit by demonstrating a range of cellular functions including inhibition of stromelysin (MMP3) and the topoisomerases,[1] induction of erythropoietin (EPO) gene expression,[15] HIF-1α protein accumulation[15] and nuclear translocation,[15] and HIF-1 DNA binding and reporter gene transactivation.[15] Pycnidione is strongly cytotoxic to human cancer cell lines (e.g., IC_{50} = 3.5 nM, HCT-116)[16] and also possesses effective antifungal,[17,18] antimalarial,[19–21] antibacterial,[17] and antithelmintic properties,[22] all in the micromolar range. Structurally homologous compounds dehydroxypycnidione (**2′**),[17] epolone A (**3′**), and epolone B (**4′**) were later isolated alongside pycnidione (**1′**),[23] and over time, a parallel collection was assembled upon the isolation of additional congeners.[24–27] While detailed structure−activity relationships have yet to be compiled, the entirety of the class maintains similar biological

activity, with bistropolones generally exhibiting the highest potency and methylation of this motif rendering the compounds inactive.[16]

All sesquiterpene-tropolones share a common 11-membered humulene-derived core displaying either pendent tropolones or phenols, but subtle features of and variations between congeners should be highlighted. Within the pycnidione series, both pycnidione (**1′**) and its deoxygenated equivalent dehydroxypycnidione (**2′**) are bistropolones, while epolone A (**3′**) and epolone B (**4′**) bear a phenol and (*E*)-trisubstituted olefin in lieu of a second tropolone, respectively. The diastereomeric eupenifeldin series maintains an identical trend among compounds but is differentiated from the former by the *syn*-relationship at the eastern dihydropyran seam (i.e., **5**−**7**) and a (*Z*)-trisubstituted olefin in the monotropolone neosetophomone B (**8**).[27] Importantly, the relative stereochemistry of both flagship members, pycnidione (**1′**) and eupenifeldin (**5**), was determined by single crystal X-ray diffraction, their absolute stereochemistry was deduced using circular dichroism studies,[1,24–27] and the absolute stereochemistry of other members within each series was assigned by analogy to **1′** and **5**.

Despite the value of their collective biological effects, no member of the sesquiterpene-tropolones has ever succumbed to total synthesis, with only the Baldwin group reporting several elegant model studies[28–33] scrutinizing a biosynthetic hypothesis (Figure 1b) insinuated in the epolone B (**4′**) isolation report.[23] It was postulated that tropolone **9** could serve as a viable precursor to the reactive tropolone *ortho*-quinone methide (*o*-QM) **10**, providing sesquiterpene-tropolones through modular [4 + 2] inverse electron demand hetero-Diels−Alder (HDA) reactions with hydroxyhumulene **11**. Thus, HDA-based union of tropolone *o*-QM **10** and the trisubstituted olefin of macrocycle **11** was envisioned to deliver epolone B (**4′**). In an identical fashion, a second HDA was anticipated to effectively transform **4′** to the corresponding biscycloadduct pycnidione (**1′**). Guided by their hypothesis, the Baldwin group conducted a proof-of-concept study (Figure 1c) by generating transient tropolone *o*-QM **10** through pyrolysis of **14** in a neat solution of *α*-humulene (**12**), observing formation of dehydroxyepolone B (**15′**) as a sole product. However, due to limited supply of *o*-QM precursor **14**, requiring 20 steps to prepare from commercial furan **13**, no further investigations involving second cycloaddition were attempted.

While this experimental evidence supported the proposed biosynthetic pathway, several key questions persisted, most importantly if hydroxyhumulene **11** was a competent partner for the cycloaddition. Recently, *in vitro* biosynthetic and computational studies by Hu and Houk successfully identified a Diels−Alderase enzyme, EupfF, responsible for the selective formation of neosetophomone B (**8**).[34] Moreover, these studies revealed the HDA reaction of **9** and **11** occurred spontaneously in the absence of EupfF (Figure 1d), generating an equimolar amount of epolone B (**4′**) and its diastereomer isoepolone B (**16′**). However, since isomeric **16′** was not previously found from producing organisms, the role of EupfF further obscures the HDA hypothesis when compared with the isolation data. It should be clarified that **11** is not a native substrate of EupfF; therefore, a separate enzyme may be operable for the selective formation of epolone B and further transformation to

pycnidione. Importantly, no biscycloadducts(i.e., **1′**, **2′**, **5**, and **6**) were detected in either case, absolving EupfF of the responsibility for this biosynthetic step. However, the Cox group has recently seen success in detecting formation of dehydroxypycnidione (**2′**) through incorporation of the PycR1 Diels−Alderase in an artificial biosynthetic pathway.[35] Finally, by refocusing on phenol-containing natural products **3′** and **7**, the same group identified enzymes responsible for a unique ring contraction of a single tropolone moiety within the bistropolone eupenifeldin (**5**), forming noreupenifeldin (**7**).[35]

Described below is our synthetic campaign toward the sesquiterpene-tropolones in the pycnidione series. We accomplished a concise and scalable preparation of several tropolone *o*-QM precursors and hydroxyhumulene. Utilizing these as cycloaddends, we conducted systematic experimental and computational investigations of their corresponding HDA reactions, resulting in the synthesis of several sesquiterpene-tropolones, and clarifying the origin of the peculiar diastereoselectivities manifest in their formation. In contrast to preceding assumptions, this research revealed that a second cycloaddition transforming epolone B to pycnidione is not a viable synthetic pathway. Moreover, we unambiguously demonstrated that the absolute stereochemical configuration of all members within the pycnidione series had previously been misassigned. Together, these studies provide a rapid and selective access to highly substituted tropolones, sesquiterpenes, and their HDA adducts, as well as foundation for their future (bio)synthetic considerations.

RESULTS AND DISCUSSION

Synthetic Planning.

The enticing modularity and brevity apparent in the biosynthetic hypothesis inspired the bio-mimicry in our synthetic blueprint toward the sesquiterpene-tropolones. While appraising the competency of hydroxylated humulene **11**, we expected this investigation of the HDA reaction to provide important insight into the biosynthesis of these unique natural products (Figure 2). Moreover, since issues with low material throughput had halted previous synthetic investigations (i.e., **14**, Figure 1c), we were adamant that the route to all cycloaddends be practical and scalable.

By favoring this modular strategy over a linear approach, the main synthetic challenge was simplified to the preparation of two cycloaddition partners, 10-hydroxyhumulene (**11**) and tropolone o-QMs (such as **17** or **18**), the latter envisioned to be formed in situ through pyrolytic cleavage of acetal precursor **19** or **20**. Inspired by de Mayo's renowned tactic,[36–38] the [2 + 2] photocycloaddition of **25** and **26** followed by base-induced fragmentation of **27** to *γ*-tropolone **28**,[39,40] we decided to explore a variation of this process that could lead to suitably functionalized *α*-tropolones (**21** → **19** or **20**). Cyclobutane **21**, which contains all desired functionality and a preinstalled halide to relay the proper tropolone oxidation state, could be traced back to intermediate **22** through an intramolecular enone-olefin [2 + 2] cycloaddition reaction.[41,42]

A tantalizing, single-step allylic oxidation of *α*-humulene (**12**) presented a direct route to **11**; however, the inherent challenges of regioselective chemical oxidation were anticipated and further supported by studies performed in our laboratories as well as others.[43] Aware

of the recent work from the Shenvi group disclosing the hydrogen atom transfer (HAT) mediated retrocycloisomerization of (−)-caryophyllene oxide (**29**) to humulene oxide **30**,[44] we envisioned an application of this methodology that might provide an alternative route toward the target molecule **11**. This advantageous disconnection would grant rapid access to the desired compound, since the appropriately hydroxylated caryophyllene oxide derivative **23** could be swiftly disconnected via α-oxidation and olefination, revealing readily available (−)-kobusone (**24**) as a suitable chiral starting material.[45,46]

Synthesis of Precursors 19 and 20.

The synthesis of *o*-QM precursors **19** and **20** commenced with *O*-alkylation of 1,3-cyclopentanedione (**31**) with the chloromethyl ether of allylic alcohol **32**, formed *in situ* with paraformaldehyde and chlorotrimethylsilane,[47] furnishing vinyl chloride **22** in 89% yield (Figure 3a). Exposure of this compound to UV irradiation promoted an intramolecular [2 + 2] cycloaddition, which delivered tricycle **33** in 74% yield as an inconsequential mixture of diastereomers (5:1). Adjustment of the oxidation state (ketone **33** → 1,2-dicarbonyl **21**) for the key fragmentation step proved troublesome. All classical α-oxidation conditions led to the decomposition of starting material, owing to the sensitivity of the tertiary chloride at the β-position. Gratifyingly, a recently reported one-pot α-iodination/Kornblum oxidation, which was used for the oxidation of cyclohexanones into catechols,[48] proved suitable for this task and delivered the desired dicarbonyl in the form of hydroxyl enone **21** in 52% yield. Having embedded all necessary functionality into the tricyclic structure **21**, we aimed to induce a de Mayo fragmentation. However, all attempts to fragment the cyclobutane ring through exposure of **21** to standard Brønsted acid or acid/base media were met with failure. Decomposition of **21** was pervasive, despite an extensive screen of reaction conditions, and in some instances we were able to detect unexpected tropolone **34**, likely formed via acetal deprotection, de Mayo fragmentation, and retro-aldol reaction.

Realizing that standard fragmentation conditions were not viable for preparation of desired tropolone **19**, we strove to identify milder conditions that would allow for retention of the 1,3-dioxane ring. The Bach group recently reported a Lewis acid mediated fragmentation (Figure 3a, inset), wherein the oxocarbenium **37**, generated from fragmentation of cyclobutane **36** by boron trifluoride diethyl etherate, was trapped by allyl- or hydrosilanes (**37** → **38**).[49] In our case, precursor **21** bears an α-proton in place of the quaternary center in **36**/**37**; thus, we postulated that, in the absence of external nucleophiles, oxocarbenium **39** could undergo deprotonation at this position, perhaps by an eliminated halide anion, restoring the 1,3-dioxane structure and bringing the seven-membered ring into a full conjugation. Fortuitously, treating **21** with excess boron trifluoride diethyl etherate induced the de Mayo type fragmentation as planned, providing tropolone **19** in 59% yield on a gram scale. To obtain unambiguous proof of the structure, the tropolone was readily crystallized from acetone and analyzed by single-crystal X-ray diffraction. While the retention of boron difluoride was unexpected after basic workup, it was not entirely surprising, as BF_2-tropolone complexes have been documented.[50] Compound **19** was remarkably bench-stable and was easily purified by silica gel chromatography or recrystallization.

While the multifaceted capability of the BF_2-group to mask the tropolone and potentially enhance the reactivity of the *o*-QM in the planned HDA reaction is of note, we also explored more traditional protecting groups, such as methoxytropolone variant **20**. Accordingly, the deprotection of tropolone difluoroborate **19** and subsequent methylation of free tropolone could be accomplished; however, this approach was plagued with low yields and delivered **20** in an inseparable mixture of constitutional isomers, one of which was inactive in the HDA reaction (see Supporting Information (SI) for detail). The hydroxyenone **21** presented a convenient opportunity to differentiate the two oxygens, and we were keen to explore alternative fragmentations of premethylated precursor **35** that could circumvent the troublesome methylation step. Intermediate **35** was readily obtained from **21** with dimethylsulfate; however, treatment with a variety of Lewis acids to effect its fragmentation as before provided only complex mixtures. At this point, alternative rearrangement pathways were explored, with attention given to the tertiary halide as a potential handle for initiating the fragmentation. Indeed, we screened silver salts and found that silver tetrafluoroborate produced **20** as the sole tropolone product in 78% yield, whose structure was also confirmed by single crystal X-ray diffraction analysis. However, our excitement about this new and improved synthesis was quickly quelled by the finding that the fragmentation was impractically slow on scales above 200 mg, and considering the requirement of stoichiometric amounts of expensive silver salt, this route was not selected for further scale-up campaigns. Nevertheless, these findings fomented a deeper exploration of the fragmentation behavior of **35** and ultimately led to the discovery that irradiation of benzene solutions with UV light (254 nm) accomplished the same conversion to **20** in 66% yield on a multigram scale. This unprecedented and direct photochemical fragmentation serves as an advantageous step with the ability to selectively generate the desired constitutional isomer of methyl tropolone **20**. Notably, photosensitizer additives had no effect, and this transformation could not be induced thermally.

Synthesis of 10-Hydroxy-*α*-humulene (11).

With tropolone *o*-QM precursors **19** and **20** in hand, we turned our focus toward the construction of 10-hydroxy-*α*-humulene (**11**, Figure 3b). While the synthesis of racemic **11** has been accomplished in 12 steps,[51] we decided to pursue the design and execution of a more streamlined, scalable, and enantioselective approach. Accordingly, the synthesis began with readily available kobusone (**24**), which was treated with potassium hexamethyldisilazane and Davis' oxaziridine,[52] furnishing hydroxyketone **40** as a single diastereoisomer (87% yield), the structure of which was confirmed by single-crystal X-ray diffraction analysis. Silyl protection of the newly formed *α*-hydroxy motif and Wittig olefination delivered key isomerization precursor **23** in 76% overall yield. Using conditions reported by Shenvi,[44] HAT-induced retrocycloisomerization of **23** proceeded smoothly to afford epoxide **41** in 95% yield, which was deprotected to alcohol **42** and verified via X-ray crystallography. The use of an epoxide to disguise the trisubstituted alkene throughout the sequence was paramount to its success, as the unmasked motif admitted unwanted side reactions under the HAT conditions. The final two steps, stereospecific Re-catalyzed deoxygenation[53] of this epoxide and silyl deprotection of the appended hydroxyl group, provided the desired macrocycle **11** in 80% overall yield, or in 73% yield if combined into a one-pot process. Importantly, while the spectroscopic data for **11** were consistent with the

literature, our synthetic sample had an opposite optical rotation compared to the material that was obtained and used in tropolone-sesquiterpene biosynthetic studies {$[\alpha]_D^{23}$ = −21.1 (c = 0.04, CH_3OH); lit.,[34] $[\alpha]_D^{20}$ = +17.5 (c = 0.04, CH_3OH)}. Finally, the described fragmentation approach to construct such a macrocycle compared favorably to alternative routes that were initially explored, involving classical ring-forming strategies used in both the synthesis of α-humulene (**12**) and other macrocycles,[54–60] such as Nozaki−Hiyama−Kishi and McMurry couplings, as well as ring-closing metathesis (see SI for details).

Dehydroxypycnidione HDA Cycloaddition Studies.

As a prelude to the biomimetic HDA reactions of **19**/**20** and **11** that we envisaged would deliver the pycnidione family of sesquiterpene-tropolones, we first profiled the cycloaddition behavior of **19**/**20** in the simpler α-humulene system demonstrated by Baldwin (Figure 4a).[30] During initial experiments, the performance of tropolone o-QM precursor **19** or **20** was evaluated by individually heating them in the presence of α-humulene (**12**). Gratifyingly, this study revealed that both **19** and **20** were competent substates for HDA reaction under microwave irradiation with **12**, generating monocycloadducts **43** (51% from **19**) and **44** (82% from **20**) as single constitutional isomers. Both sesquiterpene-tropolone products were successfully deprotected under basic conditions (K_2CO_3/MeOH, 99% yield from **43**; or NaOH, MeOH/H_2O, 80% yield from **44**) to give racemic dehydroxyepolone B (**15′**). Though a large excess (3 equiv) of tropolone o-QM precursors **19** or **20** was used to obtained practical yields, the potential bisadducts were detected only in trace amounts by LC-MS analysis of the crude reaction mixtures. These results indicated that pyrolytically generated o-QM **17** or **18** readily undergoes the first cycloaddition with humulene; however, we speculated that their rapid decomposition prevented further union with the remaining trisubstituted olefin. Moreover, during these experiments we observed pronounced decomposition of tropolone difluoroborates (i.e., **19** and **43**), which was attributed to the high temperatures required for this cycloaddition to occur. Therefore, to enforce the second cycloaddition and to avoid thermolytic degradations, the methylated monocycloadduct **44** was taken further with the corresponding o-QM precursor **20** added slowly as a solution over the course of several hours. We were pleased to find that such an approach resulted in the formation of biscycloadduct **45**, albeit with a poor yield and diastereoselectivity (13% yield and 1:1 d.r.). Separation of this diastereomeric mixture, followed by base-induced deprotection, delivered (±)-dehydroxypycnidione (**2′**).

Computed ^{13}C NMR Spectra of Dehydroxypycnidione (2′).

We were fortunate to be provided with ^{1}H NMR spectral data of dehydroxypycnidione (**2′**) from the isolation group,[17] which matched with the structure that we had synthesized. However, considering that compound **2′** was obtained as a mixture of diastereoisomers with high structural and spectroscopic homogeneity, additional characterization data, specifically the ^{13}C NMR, were crucially needed for additional structural confirmation. Thus, in lieu of the missing and unavailable data,[61] we took initiative to validate the structure of this compound by performing density functional theory (DFT) calculations to predict the ^{13}C NMR chemical shifts of **2′**.[62] After a short screening of functionals, we turned our attention to PBE0/pcSseg-2//ωB97X-D3/def2-TZVP(−f), as implemented in ORCA 4.2.1.[63–65] To our

delight, on a set of small molecules, used for empirical determination of correction factors,[66] this method displayed minor errors (MAE, mean average error = 1.2 ppm, MAX, maximum absolute error = 3.4 ppm), thus emerging as compatible with the structural elucidation of our molecules of interest. For dehydroxypycnidione (**2′**), we found satisfactory correspondence of computed model of **2′** to one of the isomers isolated in our cycloaddition.

The computed spectrum of the reported compound (Figure 4b) was compared with the experimental spectra of diastereomers synthesized in our studies. As can be seen from the graphs (Figure 4c and 4d), despite overall close correspondence (MAE = 2.2 ppm, MAX = 5.9 ppm) of the computed NMR model to the experimental spectrum, one can notice that the computational model is especially good for comparison of the aliphatic ^{13}C resonances (MAE = 1.4 ppm, MAX = 3.3 ppm), presumably due to their lower dependency on explicit solvation effects, hydrogen exchange, and/or hydrogen bonding, as compared to the tropolone units. We were able to match the distribution of resonances of aliphatic ^{13}C atoms within the error of the model and conclude the diastereomer of the naturally occurring compound reported matched one of the diastereomers we had obtained.

Epolone B and Pycnidione HDA Cycloadditions Studies.

With a practical HDA protocol established and the α-humulene series completed, we finally homed in on the critical cycloadditions with 10-hydroxyhumulene (**11**, Figure 5a). Once again, we tested both tropolone *o*-QM precursors **19** and **20** and quickly realized that BF_2-tropolone **19** was not an effective partner for the cycloaddition with **11** due to noticeable decomposition, attributed to incompatibility of the allylic alcohol with **19**. On the other hand, the application of methylated tropolone *o*-QM precursor **20** led to the desired HDA reaction, furnishing monocycloadducts **46** and **47** in 89% combined yield and with 1.4:1 diastereoselectivity. After separation of diastereoisomers, we were able to verify the configuration of **47** via X-ray analysis of its *para*-bromophenylcarbamate derivative **48**. Ultimately, base-induced deprotection of **46** and **47** delivered (+)-isoepolone B (*ent*-**16**) and (−)-epolone B (*ent*-**4**). Most of the characterization data (^1H and ^{13}C NMR, MS data) of *ent*-**16** and *ent*-**4** were consistent with those reported in the literature, but there were discrepancies in their optical rotations. The synthetic sample of (−)-epolone B (*ent*-**4**) had essentially identical but opposite optical rotation to that of the natural substance {$[\alpha]_D^{23}$ = −84.0 (*c* = 0.35, $CHCl_3$); lit.,[23] $[\alpha]_D^{23}$ = +85.0 (*c* = 0.33, CH_2Cl_2)}; thus, the synthetic compound was assigned as the unnatural enantiomer. In contrast, the synthetic sample of (+)-isoepolone B (*ent*-**16**) did not match the reported value {$[\alpha]_D^{23}$= +65.5 (*c* = 1.0, $CHCl_3$); lit.,[34] $[\alpha]_D^{20}$ = +101.3 (*c* = 0.08, $CHCl_3$)}; however, considering it was formed and isolated with (+)-epolone B (**4**) from the nonenzymatic reaction with *ent*-**11**, we assumed that our synthetic sample *ent*-**16** is the unnatural enantiomer as well.[67]

With monocycloadducts **46** and **47** in hand, the stage was set for the second cycloaddition. To our surprise, when **46** and **47** were separately taken forward for a second HDA reaction with **20**, they each produced only a single diastereomer corresponding to **51** and **49** in 24% and 26% yield, respectively. This outcome was in stark contrast to the humulene series (**44** → **45**), which gave a diastereomeric mixture, highlighting the importance of the neighboring hydroxy group on the pronounced selectivity of the second HDA. Further deprotection of **51**

and **49** led to bistropolones **52** and **50**, neither of which matched the reported spectral data of pycnidione (**1′**).[68]

This predicament left us with two options, both of which were investigated extensively: (1) correction of the stereochemistry at C10 of (−)-10-*epi*-pycnidione (**52**) to arrive at (−)-pycnidione or (2) override the inherent diastereoselectivity of the cycloaddition of **47** to provide (+)-pycnidione. However, efforts to arrive at either enantiomer of natural product were met with substantial challenges on all fronts. First, attempting to adjust the alcohol configuration on **51** or **52** through oxidation/reduction sequences with a variety of hydrides gave back only the initial **51** or **52**, and single-electron carbonyl reductions suffered from decomposition. Despite our exhaustive search for a suitable protocol, **51** and **52** were completely inert under all conditions for alcohol inversion, presumably because the necessary site of attack is buried deep within the macrocycle. The other alternative, which was to overcome the intrinsic diastereoselectivity of the second HDA reaction of **47**, also proved ineffective. The use of different hydroxy protecting groups as well as manipulation of the reaction conditions did not provide the desired stereoisomer that could lead to the target molecule (see SI for details).

Computational Studies of HDA Cycloadditions.

Faced with the remarkable yet undesired diastereoselectivity of the second cycloaddition of **20** with both monocycloadducts **46** and **47**, we sought to gain greater understanding of the factors that affect the diastereoselectivity of these transformations (Figure 5b−d). We performed DFT calculations on the *in situ* generated tropolone *o*-QM **18** with **11** to elucidate the observed selectivities at the ωB97X-D/def2-QZVPP//ωB97X-D/6–31G(d) level of theory with a CPCM(mesitylene) model for solvation.[69–73] In order to form the *S,S* and *R,R* diastereomeric products **46** and **47**, the (−)-hydroxyhumulene (**11**) must react at both faces of the dienophile. This indicates that **11** can readily access a “ring flipped” conformation, similar to the well-studied humulene system.[74,75] The lowest energy transition states **TS-1** and **TS-2** that lead to monoadducts are both *exo*, defined as the *anti*-relationship between the heterodiene and the methyl of the trisubstituted alkene (Figure 5b). The reaction barriers of **TS-1** and **TS-2** are low and primarily entropic ($\Delta G^{\ddagger}$ = 19−21 kcal·mol^{-1}), with enthalpic barriers ranging from $\Delta H^{\ddagger}$ = 5−7 kcal·mol^{-1}. These reactions will readily occur within minutes after generation of *o*-QM **18**. The difference in $\Delta G^{\ddagger}$ between **TS-1** and **TS-2** ($\Delta\Delta G^{\ddagger}$) is +0.6 kcal·mol^{-1} and indicates that **46:47** should form in a 2.8:1 ratio. When corrected for the elevated temperature (473 K), the product ratio shifts to 1.9:1, and furthermore, the experimental product ratio is well within the error of the calculation. We thoroughly evaluated popular DFT methods for the reaction and present them in the Supporting Information (see Table S1).

Adding an additional equivalent of tropolone *o*-QM **18** to react with monoadduct **46** yields a single bistropolone-sesquiterpene adduct **51**. The diastereomeric adduct (not shown) is predicted not to be observed kinetically. The transition states **TS-3** and **TS-4** have a large $\Delta\Delta G^{\ddagger}$ of 4.7 kcal·mol^{-1} (Figure 5c). We hypothesized that this noticeable difference in Gibbs free energy could be partially attributed to the hydrogen bond between the *o*-QM’s oxygen and the hydroxyl of **46**, which is present in **TS-3** (1.84 Å) but absent in **TS-4**

(3.01 Å). Similarly, the cycloadditions of **18** with **47** are predicted to yield a single diastereomer **49**. Of note, the stereochemistry of the second addition is the same in products **51** and **49**. The transition states **TS-5** and **TS-6** lead to bisadducts **49** and methylated pycnidione (**1′**), respectively (Figure 5d). The $\Delta\Delta G^{\ddagger}$ is 9.1 kcal·mol^{-1}, which indicates that formation of pycnidione by thermal HDA is not possible and a catalyst or additives must be employed. The geometries of **TS-5** and **TS-6** are strikingly different, despite having similar bond-forming distances and hydrogen bonding interactions. We hypothesize that the difference in Gibbs free energy arises from the energies of the conformations required to achieve the respective transition states, suggesting that distortion may control the reactivity. To investigate this, we stripped the monoadduct from **TS-5** and **TS-6**, optimized the geometry, and found that indeed the difference between the monoadduct conformations is 2.9 kcal·mol^{-1}, indicating that the diastereoselectivity is due in part to the energy of reactant conformations. In summary, these calculations supported the experimental outcome that the first HDA forms a mixture of diastereoisomers, but the second cycloadditions are highly stereoselective.

Revision of Absolute Stereochemistry of Pycnidione.

Based on stereochemical reassignment of epolone B (from **4′** to **4**), we postulated that the absolute stereochemistry of all natural products within the pycnidione series might be misassigned, including the flagship member pycnidione (**1′**). To set the record straight, an authentic sample of pycnidione was kindly provided by Merck Research Laboratories, identical to the material analyzed in the original isolation report.[1] The natural product was crystallized from acetonitrile, furnishing a sample suitable for X-ray analysis (Figure 6a). Upon refinement of the complete data set, several inconsistencies with the previously reported data were found. All unit cell metrics matched well (see SI, Table S7), and therefore we are highly confident in having examined the same crystal form as previously reported. Well-ordered acetonitrile molecules were observed to occupy one of the solvent accessible voids, which were not found in the previous report. The other solvent accessible void was occupied with highly disordered water molecules. The overall composition of crystal was then established as $C_{35}H_{43}NO_7{\cdot}CH_3CN{\cdot}9H_2O$, which differs from previously reported composition of $C_{35}H_{43}NO_7{\cdot}4H_2O$. Due to the substantial presence of disordered oxygen atoms, the absolute stereochemical determination using the anomalous scattering technique was complicated, as the heaviest scattering atoms on ordered molecule were also oxygen atoms. Commonly employed parameters (Flack, Hooft, Parson; see SI, Table S7) were all inconclusive of the correct absolute stereochemistry assignment. Application of Bayesian statistical analysis on the Bijvoet pair intensities allowed us to make such an assignment with high confidence.[76] The three-sided probability for incorrect absolute stereochemistry was determined to be 10^{-4}, and the probability of racemic twinning, to be 10^{-34}. Thus, given the X-ray anomalous scattering data, our best hypothesis is that the correct absolute stereochemical model belongs in the $P6_1$ (# 169), and not in its enantiomorphic $P6_5$ (# 170) space group.

In order to corroborate our conclusions about the absolute stereochemistry from the single crystal XRD experiment, we decided to calculate the electronic circular dichroism transitions and compare them to the originally reported data (Figure 6b and 6c). We

obtained TD-DFT transition energies with single-point ωB97X/def2-TZVP calculation with the CPCM(Ethanol) implicit solvation model on unoptimized geometry from our XRD experiment (see SI for details). According to the original report, positive and negative peaks should be observed at 260 and 238 nm, respectively, which perfectly matches the predicted spectrum for a molecular geometry which is enantiomeric to that proposed in the literature. Performing an analogous computation on the X-ray geometry from the literature, we arrived at the spectrum which was, expectedly so, inverted vertically and hence displays a complete mismatch with the literature report. It should be noted that the original absolute stereochemistry proposal was made based on the ECD interpretation, which the present computational data do not corroborate. Having examined both the anomalous scattering data and the ECD data, we have high confidence that the absolute stereochemistry of pycnidione was incorrectly determined.

Alternative Biosynthetic Considerations.

The synthetic studies described above, supported by the computational data and stereochemical reassignments, shine additional light on the biogenesis of the sesquiterpene-tropolones (Figure 7). Thus, α-humulene (**12**) undergoes oxidation to (+)-(10*R*)-hydroxyhumulene (*ent*-**11**) followed by HDA reaction with tropolone *o*-QM **10** to give epolone B (**4**) and isoepolone B (**16**). While these transformations were already reported during the eupenifeldin biosynthetic studies by Hu and co-workers (Figure 1d),[34] our asymmetric total synthesis (**11** → **46** + **47**, Figure 5a) led to reassignment of absolute stereochemistry of all cycloaddition components (*ent*-**11**, **4**, and **16**). On the other hand, although there are no biosynthetic studies of a second HDA in native producers, our synthetic campaign unveiled the formation of sesquiterpenes-bistropolones (**51** and **49**, Figure 5a) relevant to the proposed biosynthesis. Notably, the second HDA with epolone B (**4**) revealed remarkable macrocyclic stereocontrol, with peripheral attack of the *o*-QM occurring at the diastereoface opposite to that which leads to pycnidione (**1**). These observations, supported by DFT computational data, provide strong evidence that nonenzymatic conversion of **4** to **1** is not feasible. Therefore, we speculate two different possibilities for the formation of pycnidione (**1**). First, separate enzymes may exist that assist in the second cycloaddition process (**4** → **1**), as also proposed by Hu. Alternatively, the formation of pycnidione (**1**) could be achieved through a late-stage enzymatic C−H oxidation of dehydroxypycnidione (**2**). That in turn could be formed from α-humulene (**12**) and double HDA, involving dehydroxyepolone B (**15**) as an intermediate, as both have been readily formed during our synthetic studies. We are quick to note, however, that this is not in line with literature precedent, as **15** has never been isolated and **2** has only once been coisolated from mixtures containing **1**, and therefore our proposal is merely speculative. Finally, since the second HDA between **10** and **4** or **16** is spontaneous and synthetically feasible, as demonstrated with the preparation of bistropolones **50** and **52**, it is possible that these compounds are in fact bona fide sesquiterpene-bistropolone natural products still awaiting discovery within natural sources (as *ent*-**50** and *ent*-**52**).

CONCLUSION

Concise, modular, and efficient total syntheses of sesquiterpene-tropolones have been developed, which unravel many chemical and biosynthetic characteristics of this structurally unique class of macrocyclic meroterpenoids. Within the described routes to key HDA partners hydroxyhumulene (**11**) and *o*-QM precursors (**19** and **20**), radical-based assembly and fragmentation of intermediates served as a common theme. Of note is a novel, photochemical-based method to generate tropolones that is complementary to de Mayo fragmentation and may find application in the selective construction of other tropolone-containing natural products. Likewise, the requisite hydroxyhumulene was prepared in a rapid and practical fashion from chiral pool starting material. The robustness of the chosen routes permitted assembly of all key building blocks on a gram to decagram scale and enabled comprehensive investigations of their union through HDA chemistry. Biomimetic cycloaddition studies produced several natural products, including (−)-epolone B (*ent*-**4**), (+)-isoepolone B (*ent*-**16**), and (±)-dehydroxypycnidione (**2**). Furthermore, two new sesquiterpene bistropolones 8,9-*epi*,*epi*-(+)-pycnidione (**50**) and 10-*epi*-(−)-pycnidione (**52**) were formed in highly selective HDA reactions from *ent*-**4** and *ent*-**16**. Computational modeling effectively explained the origins of selectivities observed in the HDA reactions. These studies uncover stereochemical inconsistencies and consequently merited structural reinvestigation of natural pycnidione (**1**), resulting in stereochemical reassignments of all natural products within the pycnidione series.

These endeavors also secured additional insight into the biogenesis of these metabolites. The previously assumed biomimetic pathway from epolone B (**4**) to pycnidione (**1**) is not viable through spontaneous HDA-assembling mechanisms, in contrast to nonenzymatic cycloaddition leading to epolone B (**4**). Further biosynthetic studies will be required to uncover the potential role of enzymatic involvement in the second HDA, or in any alternative pathways leading to formation of **1**. Likewise, additional synthetic studies are warranted to reach pycnidione and to explore the chemical biology and medicinal chemistry of these unique metabolites. The HDA stratagem described above may be adapted to afford various analogues of sesquiterpene-tropolones and can also be useful for the synthesis of other natural products, including members of the eupenifeldin series.

Supplementary Material

Refer to Web version on PubMed Central for supplementary material.

ACKNOWLEDGMENTS

Financial support for this work was provided by the University of Illinois and National Institute of General Medical Sciences, National Institute of Health (GM 124480 to K.N.H.). Bristol Myers Squibb, Amgen, Eli Lilly, and FMC are also acknowledged for unrestricted research support. The Bruker 500-MHz NMR spectrometer was obtained with the financial support of the Roy J. Carver Charitable Trust, Muscatine, Iowa, USA. We also thank Dr. D. Olson and Dr. L. Zhu for NMR spectroscopic assistance, Dr. D. L. Gray and Dr. T. Woods for X-ray crystallographic analysis assistance, and F. Sun for mass spectrometric assistance. We thank Dr. Patrick S. Fier (Merck Research Laboratories) for providing us with an authentic sample of pycnidione and Dr. Russel G. Kerr (University of Prince Edward Island) for sharing their NMR data of dehydroxypycnidione. Finally, we would like to thank Matthew Bock and Yingzhe Yang for assistance with this work and Christopher J. Huck for critical proofreading of this paper. We dedicate this work in memory of Sir Jack Baldwin.

REFERENCES

(1). Harris GH; Hoogsteen K; Silverman KC; Raghoobar SL; Bills GF; Lingham RB; Smith JL; Dougherty HW; Cascales C; Pelaez F Isolation and Structure Determination of Pycnidione, a Novel Bistropolone Stromelysin Inhibitor from a Phoma sp. Tetrahedron 1993, 49, 2139–2144.

(2). For examples of related natural products, see refs 2–6.Ito T Fusariocin C, a New Cytotoxic Substance Produced by Fusarium-Moniliforme. Agric. Biol. Chem 1979, 43, 1237–1242.

(3). Park SY; Choi H; Hwang H; Kang H; Rho J-R Gukulenins A and B, Cytotoxic Tetraterpenoids from the Marine Sponge Phorbas gukulensis. J. Nat. Prod 2010, 73, 734–737. [PubMed: 20232859]

(4). Angawi RF; Swenson DC; Gloer JB; Wicklow DT Malettinin A: A New Antifungal Tropolone from an Unidentified Fungal Colonist of Hypoxylon Stromata (NRRL 29110). Tetrahedron Lett. 2003, 44, 7593–7596.

(5). Silber J; Ohlendorf B; Labes A; Wenzel-Storjohann A; Nather C; Imhoff JF Malettinin E, an Antibacterial and Anti Fungal Tropolone Produced by a Marine Cladosporium strain. Front. Mar. Sci 2014, 35, 1–6.

(6). Angawi RF; Swenson DC; Gloer JB; Wicklow DT Malettinins B-D: New Polyketide Metabolites from an Unidentified Fungal Colonist of Hypoxylon stromata (NRRL 29110). J. Nat. Prod 2005, 68, 212–216. [PubMed: 15730245]

(7). For examples of synthetic tropolone products and relevant studies, see refs 7–14.Yamato M; Hashigaki K; Kokubu N; Tsuruo T; Tashiro T Synthesis and Antitumor Activity of Tropolone Derivatives. J. Med. Chem 1984, 27, 1749–1753. [PubMed: 6502608]

(8). Yamato M; Hashigaki K; Ishikawa S; Kokubu N; Inoue Y; Tashiro T Synthesis and Antitumor Activity of Tropolone Derivatives. J. Med. Chem 1985, 28, 1026–1031. [PubMed: 4020825]

(9). Yamato M; Hashigaki K; Kokubu N; Tashiro T; Tsuruo T Synthesis and Antitumor Activity of Tropolone Derivatives. J. Med. Chem 1986, 29, 1202–1205. [PubMed: 3806570]

(10). Yamato M; Hashigaki K; Sakai J; Kawasaki Y; Tsukagoshi S; Tashiro T Synthesis and Antitumor Activity of Tropolone Derivatives. J. Med. Chem 1987, 30, 117–120. [PubMed: 3806588]

(11). Yamato M; Hashigaki K; Sakai J; Takeuchi Y; Tsukagoshi S; Tashiro T; Tsuruo T Synthesis and Antitumor Activity of Tropolone Derivatives. J. Med. Chem 1987, 30, 1245–1248. [PubMed: 3599030]

(12). Yamato M; Hashigaki K; Yasumoto Y; Sakai J; Luduena RF; Banerjee A; Tsukagoshi S; Tashiro T; Tsuruo T Synthesis and Antitumor Activity of Tropolone Derivatives. Structure-Activity Relationships of Antitumor-Active Tropolone and 8-Hydroxyquino-line Derivatives. J. Med. Chem 1987, 30, 1897–1900. [PubMed: 3116257]

(13). Yamato M; Ando J; Sakaki K; Hashigaki K; Wataya Y; Tsukagoshi S; Tashiro T; Tsuruo T Synthesis and Antitumor Activity of Tropolone Derivatives. Bistropolones Containing Connecting Methylene Chains. J. Med. Chem 1992, 35, 267–273. [PubMed: 1732542]

(14). Yamato M; Hirota Y; Yoshida S; Tanaka S; Morita T; Sakai J; Hashigaki K; Hayatsu H; Wataya Y Imbalance of Deoxyribonucleoside Triphosphates and DNA Double-strand Breaks in Mouse Mammary Tumor FM3A Cells Treated *in vitro* with an Antineoplastic Tropolone Derivative. Jpn. J. Cancer Res 1992, 83, 661–668. [PubMed: 1644668]

(15). Hsiao C-J; Hsiao S-H; Chen W-L; Guh J-H; Hsiao G; Chan Y-J; Lee T-H; Chung C-L Pycnidione, a Fungus-Derived Agent, Induces Cell Cycle Arrest and Apopotosis in A549 Human Lung Cancer Cells. Chem.-Biol. Interact 2012, 197, 23–30. [PubMed: 22450442]

(16). Kaneko M; Matsuda D; Ohtawa M; Fukuda T; Nagamitsu T; Yamori T; Tomoda H Potentiation of Bleomycin in Jurkat Cells by Fungal Pycnidione. Biol. Pharm. Bull 2012, 35, 18–28. [PubMed: 22223332]

(17). For antifungal properties, see refs 17 and 18.Overy DP; Berrue F; Correa H; Hanif N; Hay K; Lanteigne M; Mquilian K; Duffy S; Boland P; Jagannathan R; Carr GS; Vansteeland M; Kerr RG Sea foam as a Source of Fungal Inoculum for the Isolation of Biologically Active Natural Products. Mycology 2014, 5, 130–144. [PubMed: 25379337]

(18). Kerr RG; Overy DP; Berué F Anti-Dandruff Composition Comprising Pycnidione and Epolone. PCT Int. Appl. WO2016/198848, 2016.

(19). For antimalarial properties, see refs 19–21.Höller U; Wright AD; Matthée GF; Konig GM; Draeger S; Aust H-J; Schulz B Fungi from marine sponges: diversity, biological activity and secondary metabolites. Mycol. Res 2000, 104, 1354–1365.

(20). Wright AD; Lang-Unnasch N Potential Antimalarial Lead Structures from Fungi of Marine Origin. Planta Med. 2005, 71, 964–966. [PubMed: 16254832]

(21). Pittayakhajonwut P; Theerasilp M; Kongsaeree P; Rungrod A; Tanticharoen M; Thebtaranonth Y Pughiinin A, a Sesquiterpene from the Fungus *Kionochaeta pughii* BCC 2878. Planta Med. 2002, 68, 1017–1019. [PubMed: 12451493]

(22). Ayers S; Zink DL; Powell JS; Brown CM; Grund A; Bills GF; Platas G; Thompson D; Singh SB Noreupenifeldin, a Tropolone from an Unidentified Ascomycete. J. Nat. Prod 2008, 71, 457–459. [PubMed: 18095654]

(23). Cai P; Smith D; Cunningham B; Brown-Shimer S; Katz B; Pearce C; Venables D; Houck D Epolones: Novel Sesquiterpene-Tropolones from Fungus OS-F69284 That Induce Erythropoietin in Human Cells. J. Nat. Prod 1998, 61, 791–795. [PubMed: 9644066]

(24). For eupenifeldin isolation, see refs 24 and 25.Mayerl F; Gao Q; Huang S; Klohr SE; Matson JA; Gustavson DR; Pirnik DM; Berry RL; Fairchild C; Rose WC Eupenifeldin, A Novel Cytotoxic Bistropolone From *Eupenicillium brefeldianum*. J. Antibiot 1993, 46, 1082–1088.

(25). Gao Q; Mayerl F Eupenifeldin. Acta Crystallogr., Sect. C: Cryst. Struct. Commun 1994, 50, 2033–2036.

(26). For noreupenifeldin isolation, see:Ayers S; Zink DL; Powell JS; Brown CM; Grund A; Bills GF; Platas G; Thompson D; Singh SB Noreupenifeldin, a Tropolone from an Unidentified Ascomycete. J. Nat. Prod 2008, 71, 457–459. [PubMed: 18095654]

(27). For dehydroxyeupenifeldin and neosetophomone B isolations, see:El-Elimat T; Raja HA; Ayers S; Kurina SJ; Burdette JE; Mattes Z; Sabatelle R; Bacon JW; Colby AH; Grinstaff MW; Pearce CJ; Oberlies NH Meroterpenoids from *Neosetophoma* sp.: A Dioxa[4.3.3]propellane Ring System, Potent Cytotoxicity, and Prolific Expression. Org. Lett 2019, 21, 529–534. [PubMed: 30620608]

(28). For previous model studies, see refs 28–33.Baldwin JE; Mayweg AVW; Neumann K; Pritchard GJ Studies toward the Biomimetic Synthesis of Tropolone Natural Products via Hetero Diels–Alder Reaction. Org. Lett 1999, 1, 1933–1935. [PubMed: 10905860]

(29). Adlington RM; Baldwin JE; Pritchard GJ; Williams AJ; Watkin DJ A Biomimetic Synthesis of Lucidene. Org. Lett 1999, 1, 1937–1939. [PubMed: 10905861]

(30). Adlington RM; Baldwin JE; Pritchard GJ; Mayweg AVW; Pritchard GJ Biomimetic Cycloaddition Approach to Tropolone Natural Products *via* a Tropolone Ortho-quinone Methide. Org. Lett 2002, 4, 3009–3011. [PubMed: 12182611]

(31). Baldwin JE; Mayweg AVW; Pritchard GJ; Adlington RM Expedient Synthesis of a Highly Substituted Tropolone via 3-oxidopyrylium [5 + 2] Cycloaddition Reaction. Tetrahedron Lett 2003, 44, 4543–4545.

(32). Rodriguez R; Adlington RM; Moses JE; Cowley A; Baldwin JE A New and Efficient Method for *o*-Quinone Methide Intermediate Generation: Application to the Biomimetic Synthesis of (±)-Alboatrin. Org. Lett 2004, 6, 3617–3619. [PubMed: 15387562]

(33). Rodriguez R; Moses JE; Adlington RM; Baldwin JE A New and Efficient Method for *o*-Quinone Methide Intermediate Generation: Application to the Biomimetic Synthesis of Benzopyran Derived Natural Products (±)-Lucidene and (±)-Alboatrin. Org. Biomol. Chem 2005, 3, 3488–3495. [PubMed: 16172685]

(34). Chen Q; Gao J; Jamieson C; Liu J; Ohashi M; Bai J; Yan D; Liu B; Che Y; Wang Y; Houk KN; Hu Y Enzymatic Intermolecular Hetero-Diels–Alder Reaction in the Biosynthesis of Tropolonic Sesquiterpenes. J. Am. Chem. Soc 2019, 141, 14052–14056. [PubMed: 31461283]

(35). Schotte C; Li L; Wibberg D; Kalinowski J; Cox RJ Synthetic Biology Driven Biosynthesis of Unnatural Tropolone Sesquiterpenoids. Angew. Chem., Int. Ed 2020, 59, 23870–23878.

(36). For reviews, see refs 36–38.De Mayo P Photochemical Syntheses. 37. Enone Photoannelation. Acc. Chem. Res 1971, 4, 41–47.

(37). Oppolzer W The Intramolecular [2 + 2] Photoaddition/Cyclobutane-Fragmentation Sequence in Organic Synthesis. Acc. Chem. Res 1982, 15, 135–141.

(38). Winkler JD; Bowen C Mazur.; Liotta, Fina. [2 + 2] Photocycloaddition/Fragmentation Strategies for the Synthesis of Natural and Unnatural Products. Chem. Rev 1995, 95, 2003–2020.

(39). Lange GL; de Mayo P Photochemical Synthesis: Stipitotanic Acid. Chem. Commun 1967, 704.

(40). Challand BD; Hikino H; Kornis G; Lange G; de Mayo P Photochemical Cycloaddition. Some Applications of the Use of Enolized β–Diketones. J. Org. Chem 1969, 34, 794–806.

(41). For reviews, see refs 41 and 42.Crimmins MT; Reinhold TL Enone Olefin [2 + 2] Photochemical Cycloadditions. Org. React 1993, 44, 297.

(42). Poplata S; Tröster A; Zou Y-Q; Bach T Recent Advances in the Synthesis of Cyclobutanes by Olefin [2 + 2] Photocycloaddition Reactions. Chem. Rev 2016, 116, 9748–9815. [PubMed: 27018601]

(43). Zigon N; Hoshino M; Yoshioka S; Inokuma Y; Fujita M Where is the Oxygen? Structural Analysis of α-Humulene Oxidation Products by the Crystalline Sponge Method. Angew. Chem., Int. Ed 2015, 54, 9033–9037.

(44). Crossley SWM; Barabé F; Shenvi RA Simple, Chemoselective, Catalytic Olefin Isomerization. J. Am. Chem. Soc 2014, 136, 16788–16791. [PubMed: 25398144]

(45). Kobusone can be readily synthesized from commercially available caryophyllene oxide in a single step:Bume DD; Pitts CR; Ghorbani F; Harry SA; Capilato JN; Siegler MA; Lectka T Ketones as Directing Groups in Photocatalytic sp^3 C-H Fluorination. Chem. Sci 2017, 8, 6918–6923. [PubMed: 29147517]

(46). For a recent review on chiral pool starting materials for terpene synthesis, see:Brill ZG; Condakes ML; Ting CP; Maimone TJ Navigating the Chiral Pool in the Total Synthesis of Complex Terpene Natural Products. Chem. Rev 2017, 117, 11753–11795. [PubMed: 28293944]

(47). Bairamov GI Synthesis of New Nitrogen-Containing Compounds on the Basis of 2,6-Dichloro-5-oxo-2-hexene and Their Study. Azerb. Khim. Zh 2008, 3, 174–180.

(48). Liang Y-F; Li X; Wang X; Zou M; Tang C; Liang Y; Song S; Jiao N Conversion of Simple Cyclohexanones into Catechols. J. Am. Chem. Soc 2016, 138, 12271–12277. [PubMed: 27564642]

(49). Brimioulle R; Bach T [2 + 2] Photocycloaddition of 3-Alkenyloxy-2-cycloalkenones: Enantioselective Lewis Acid Catalysis and Ring Expansions. Angew. Chem., Int. Ed 2014, 53, 12921–12924.

(50). Sato M; Ebine S; Tsunetsugu J Small Ring-annelated Non-benzenoid Aromatic Compounds: 1,2-Dihydrocyclobuta[*e*]tropolone. J. Chem. Soc., Chem. Commun 1978, 215.

(51). Takahashi T; Kitamura K; Tsuji J Synthesis of New Humulene Derivatives; (2*E*,6*E*,9*E*)-Cycloundecatrienones, by Intramolecular Alkylation of Protected Cyanohydrin. A Route to Humulene. Tetrahedron Lett. 1983, 24, 4695–4698.

(52). Davis FA; Vishwakarma LC; Billmers JG; Finn J Synthesis of.Alpha.-Hydroxycarbonyl Compounds (Acyloins): Direct Oxidation of Enolates Using 2-Sulfonyloxaziridines. J. Org. Chem 1984, 49, 3241–3243.

(53). Nakagiri T; Murai M; Takai K Stereospecific Deoxygenation of Aliphatic Epoxides to Alkenes under Rhenium Catalysis. Org. Lett 2015, 17, 3346–3349. [PubMed: 26065934]

(54). For classic strategies for the synthesis of α-humulene, see refs 54–60.Corey EJ; Hamanaka E. Total Synthesis of Humulene. J. Am. Chem. Soc 1967, 89, 2758–2759.

(55). Vig OP; Ram B; Atwal KS; Bari SS Terpenoids. 125. New Synthesis of Humulene (2,6,6,9-tetramethylcycloundeca-1,4,8-triene). Indian J. Chem 1976, 14B, 855–857.

(56). Kitagawa Y; Itoh A; Hashimoto S; Yamamoto H; Nozaki H Total Synthesis of Humulene. A Stereoselective Approach. J. Am. Chem. Soc 1977, 99, 3864–3867.

(57). McMurry JE; Matz JR Stereospecific Synthesis of Humulene by Titanium-Induced Dicarbonyl Coupling. Tetrahedron Lett. 1982, 23, 2723–2724.

(58). Miyaura N; Suginome H; Suzuki A New Stereo- and Regiospecific Synthesis of Humulene by Means of the Palladium-Catalyzed Cyclization of Haloalkenylboranes. Tetrahedron Lett. 1984, 25, 761–764.

(59). Corey EJ; Daigneault S; Dixon BR A Biomimetic Chemical Synthesis of Humulene from Farnesol. Tetrahedron Lett. 1993, 34, 3675–3678.

(60). Hu T; Corey EJ Short Syntheses of (±)-δ-Araneosene and Humulene Utilizing a Combination of Four-Component Assembly and Palladium-Mediated Cyclization. Org. Lett 2002, 4, 2441–2443. [PubMed: 12098267]

(61). Though dehydroxypycnidione was recently reported to be isolated through combinatorial biosynthesis (ref 35), the reported spectroscopic data for this natural product did not match our data as well as data provided to us by the initial isolation group.

(62). Boyko YD; Huck CJ; Ning S; Shved AS; Yang C; Chu T; Tonogai EJ; Hergenrother PJ; Sarlah D Synthetic Studies on Selective, Proapoptotic Isomalabaricane Triterpenoids Aided by Computational Techniques. J. Am. Chem. Soc 2021, 143, 2138–2155. [PubMed: 33464048]

(63). Neese F Software Update: The ORCA Program System, Version 4.0. Wiley Interdiscip. Rev.: Comput. Mol. Sci 2018, 8, e1327.

(64). Neese F The ORCA Program System. Wiley Interdiscip. Rev.: Comput. Mol. Sci 2012, 2, 73–78.

(65). Jensen F Segmented Contracted Basis Sets Optimized for Nuclear Magnetic Shielding. J. Chem. Theory Comput 2015, 11, 132–138. [PubMed: 26574211]

(66). Lodewyk MW; Siebert MR; Tantillo DJ Computational Prediction of 1 H and 13 C Chemical Shifts: A Useful Tool for Natural Product, Mechanistic, and Synthetic Organic Chemistry. Chem. Rev 2012, 112, 1839–1862. [PubMed: 22091891]

(67). Based on this data, the naturally obtained isoepolone B (**16**) should have the negative optical rotation value.

(68). Oxidation of **51** with DMP delivered the ketone that spectroscopically (^{1}H and ^{13}C NMR) matched with oxidized and methylated natural pycnidione.

(69). Chai J-D; Head-Gordon M Long-Range Corrected Hybrid Density Functionals with Damped Atom–Atom Dispersion Corrections. Phys. Chem. Chem. Phys 2008, 10, 6615–6620. [PubMed: 18989472]

(70). Weigend F; Ahlrichs R Balanced Basis Sets of Split Valence, Triple Zeta Valence and Quadruple Zeta Valence Quality for H to Rn: Design and Assessment of Accuracy. Phys. Chem. Chem. Phys 2005, 7, 3297–3305. [PubMed: 16240044]

(71). Hehre WJ; Ditchfield R; Pople JA Self–Consistent Molecular Orbital Methods. XII. Further Extensions of Gaussian–Type Basis Sets for Use in Molecular Orbital Studies of Organic Molecules. J. Chem. Phys 1972, 56, 2257–2261.

(72). Hariharan PC; Pople JA The Influence of Polarization Functions on Molecular Orbital Hydrogenation Energies. Theor. Chim. Acta 1973, 28, 213–222.

(73). Grimme S; Antony J; Ehrlich S; Krieg H A Consistent and Accurate Ab Initio Parametrization of Density Functional Dispersion Correction (DFT-D) for the 94 Elements H-Pu. J. Chem. Phys 2010, 132, 154104. [PubMed: 20423165]

(74). Shirahama H; Osawa E; Matsumoto T Conformational Studies on Humulene by Means of Empirical Force Field Calculations. Role of Stable Conformers of Humulene in Biosynthetic and Chemical Reactions. J. Am. Chem. Soc 1980, 102, 3208–3213.

(75). Neuenschwander U; Czarniecki B; Hermans I Origin of Regioselectivity in α-Humulene Functionalization. J. Org. Chem 2012, 77, 2865–2869. [PubMed: 22332847]

(76). Hooft RWW; Straver LH; Spek AL Determination of Absolute Structure Using Bayesian Statistics on Bijvoet Differences. J. Appl. Crystallogr 2008, 41, 96–103. [PubMed: 19461838]

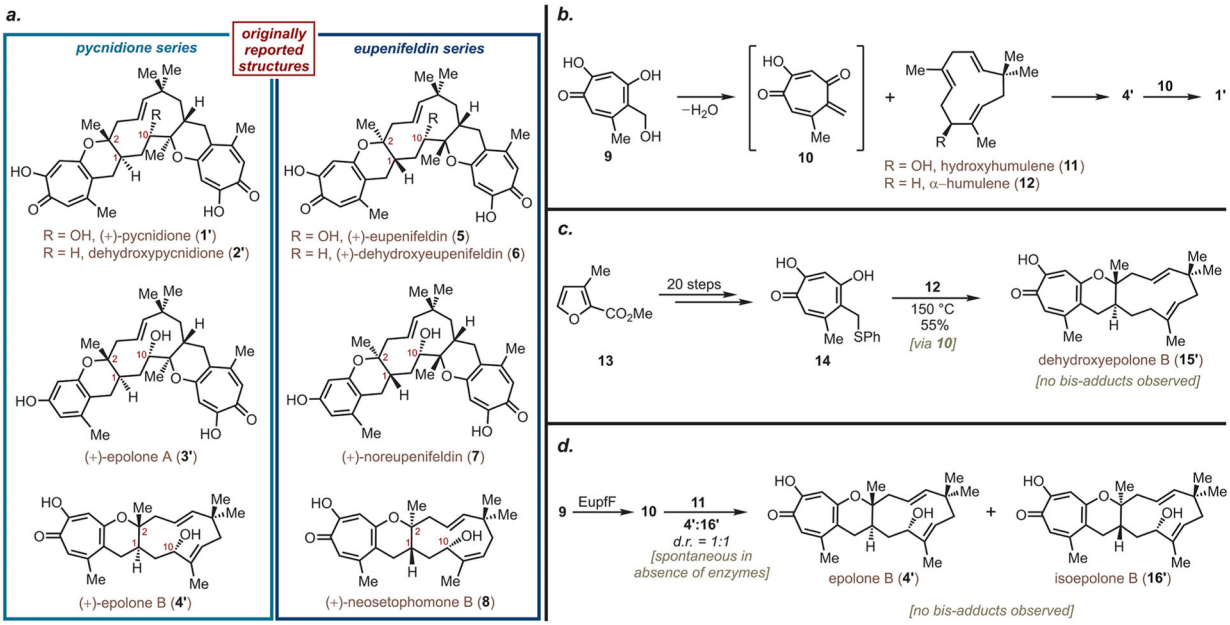

Figure 1.

(a) Originally reported structures of representative members of the sesquiterpene-tropolones belonging to the pycnidione and eupenifeldin series. (b) Biosynthetic proposal for pycnidione series. (c) Prior key synthetic studies. (d) Biosynthetic studies of epolone B (**4′**).

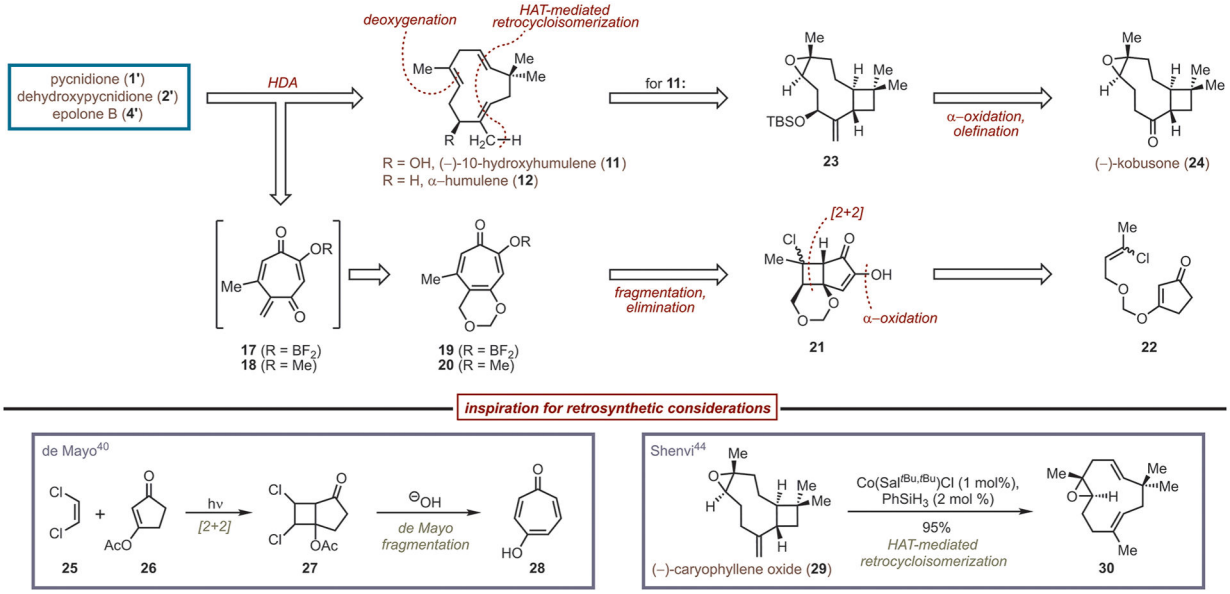

Figure 2.

Retrosynthetic analysis of pycnidione (**1′**), dehydroxypycnidione (**2′**), and epolone B (**4′**).

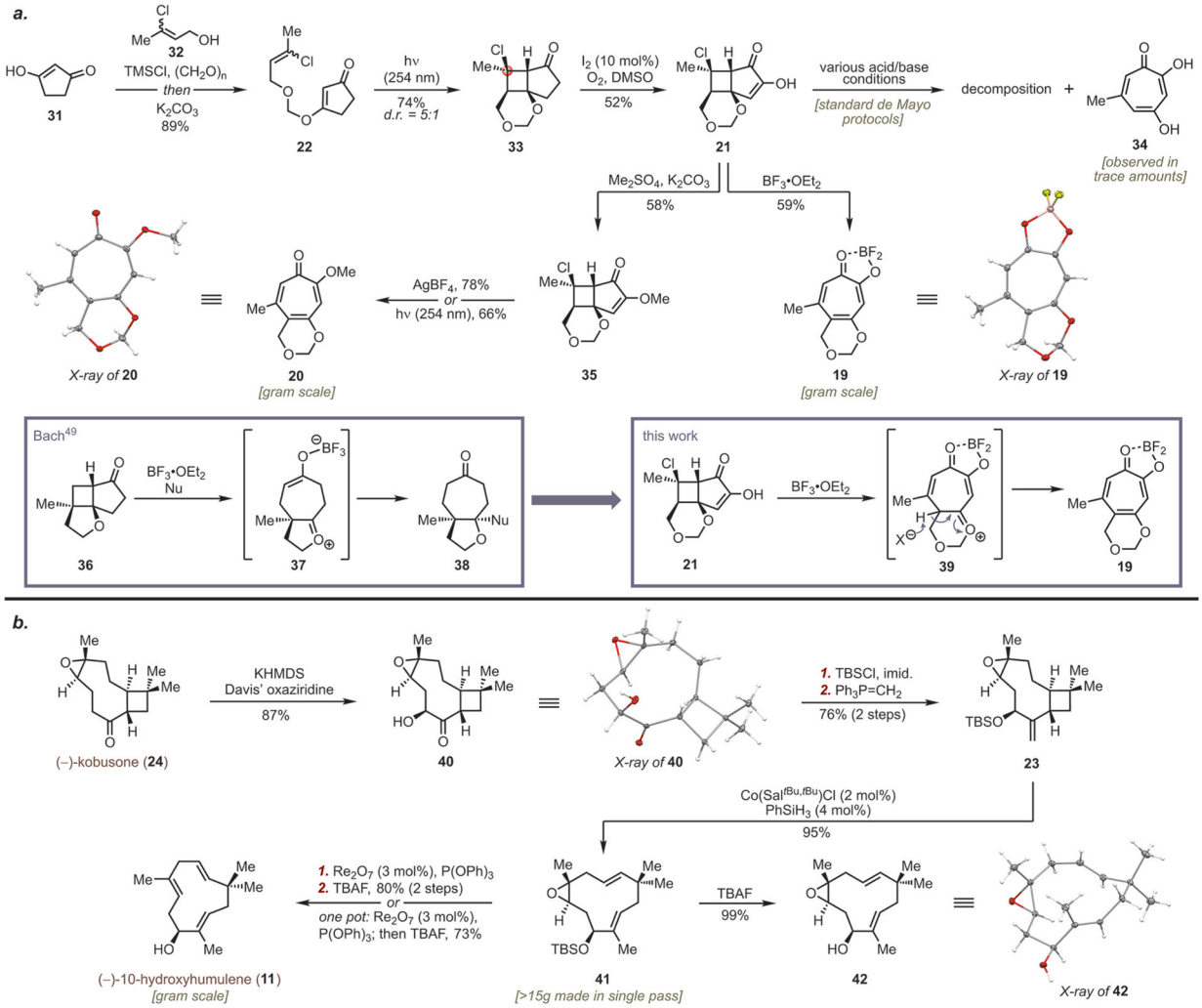

Figure 3.

Preparation of HDA cycloaddition partners. (a) Synthesis of tropolones **19** and **20**. (b) Synthesis of 10-hydroxy-α-humulene (**11**).

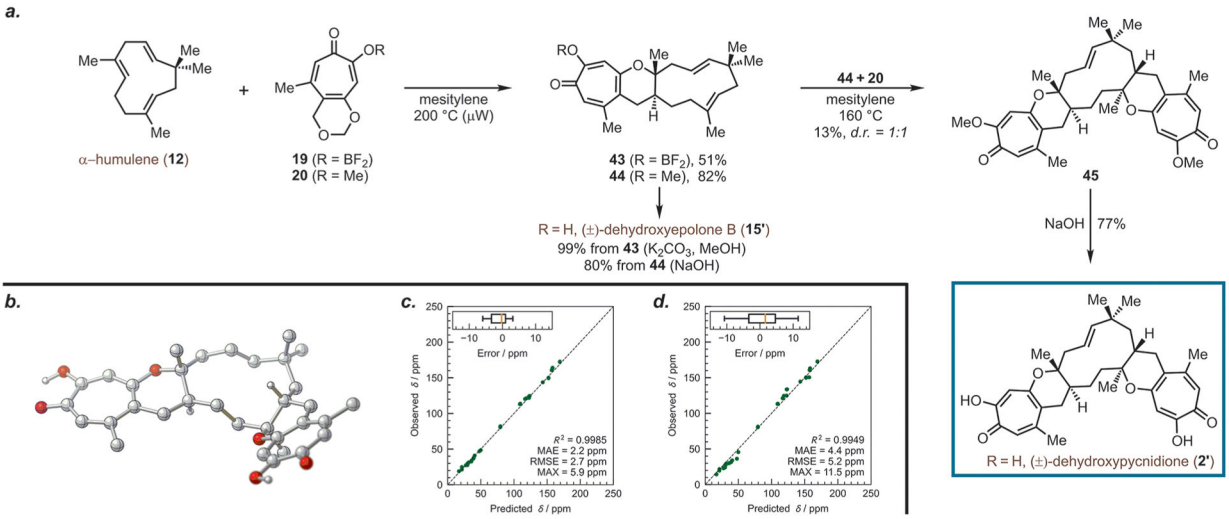

Figure 4.

(a) HDA cycloaddition studies involving α-humulene (**12**) and synthesis of dehydroxypycnidione (**2′**). (b) Optimized geometry of **2′** and (c and d) scatter plots of predicted ^{13}C NMR shifts of **2′** as compared to both observed diastereoisomers. Insets correspond to error distributions. Diagonal dashed line: $y = x$.

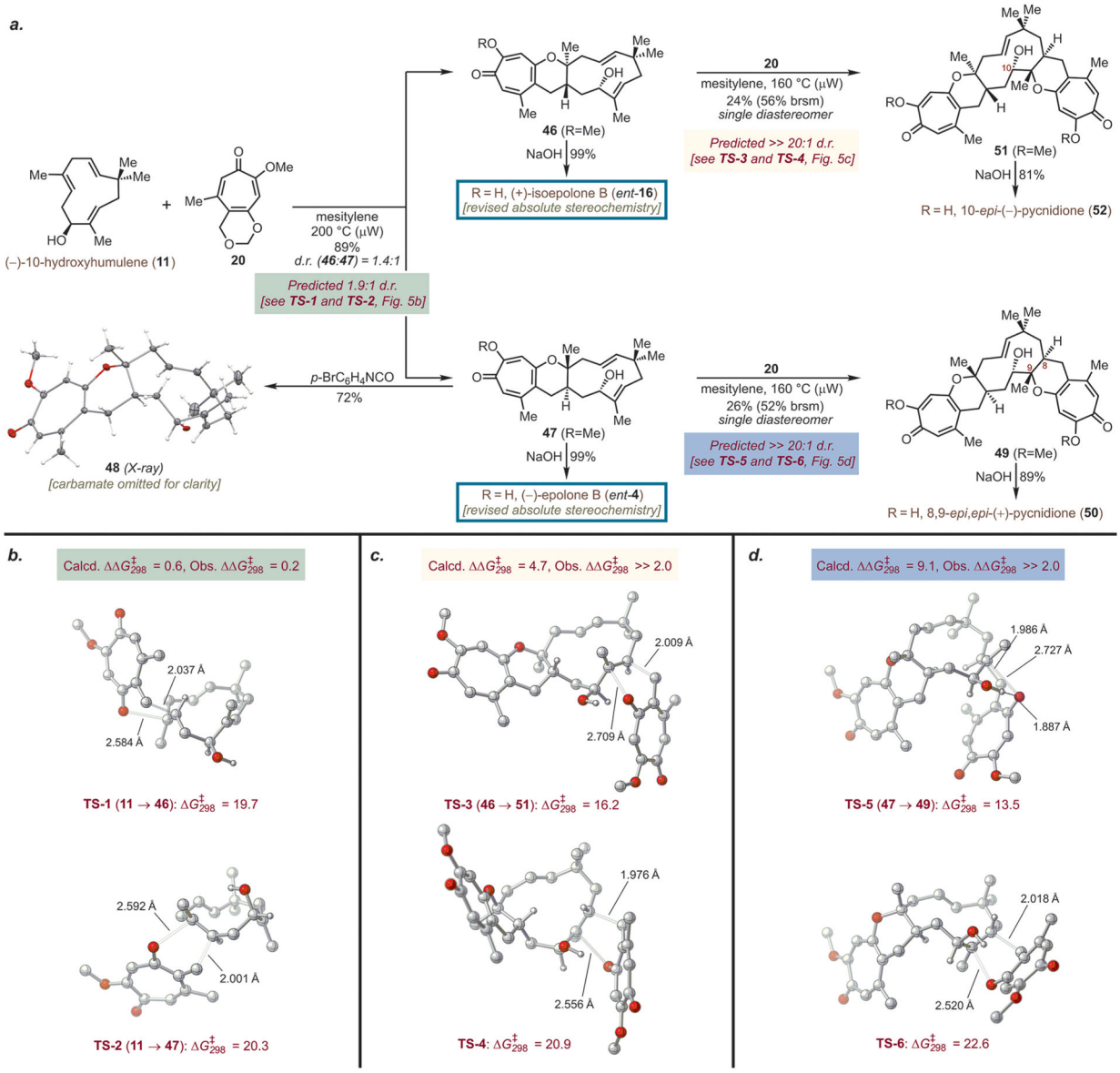

Figure 5.

(a) HDA cycloaddition studies involving (−)-10-hydroxyhumulene (**11**) and synthesis of (+)-isoepolone B (*ent*-**16**) and (−)-epolone B (*ent*-**4**). (b) Computed transition state (TS) energies for the reaction of **11** and **20** to form **46** and **47**. (c) Computed TS energies for the reaction of **20** and **46**. (d) Computed TS energies for the reaction of **20** and **47**. Calculations with ωB97X-D-CPCM(Mesitylene)/def2-QZVPP//ωB97X-D/6–31G(d).

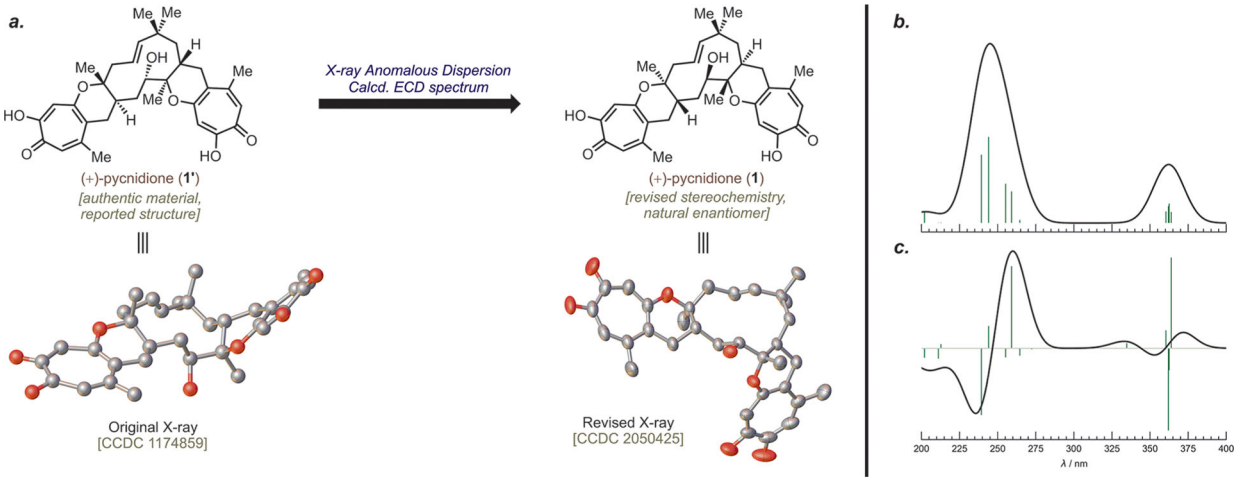

Figure 6.

(a) Structural reinvestigation of authentic sample of (+)-pycnidione (**1**). (b) TD-DFT/ωB97X/def2-TZVP electronic transitions, plotted with UV/vis intensities (green lines). (c) TD-DFT transitions plotted with ECD intensities.

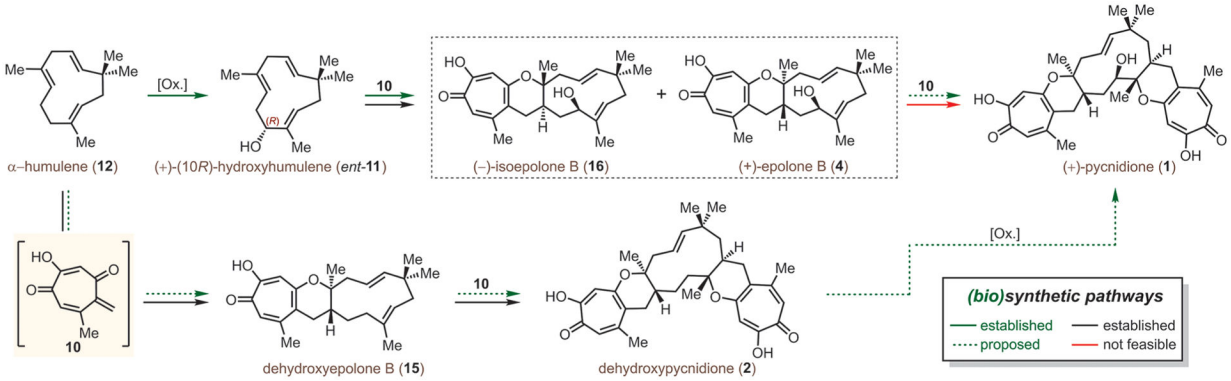

Figure 7.
Updated (bio)synthetic pathways of pycnidione series.